JOC Article
pubs.acs.org/joc

The Reactivity of the 1,4-Biradical Formed by Norrish Type Reactions of Aqueous Valerophenone: A QM/MM-Based FEP Study

Lin Shen and Wei-Hai Fang*

College of Chemistry, Beijing Normal University, Beijing 100875, China

fangwh@bnu.edu.cn

Received September 11, 2010

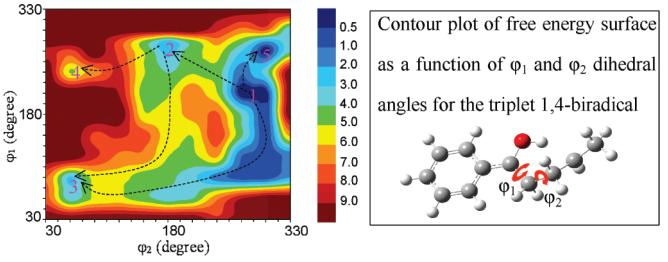

In the present work, Norrish type reactions of aqueous valerophenone and the reactivity of the triplet 1,4-biradical formed by the 1,5-H shift have been studied with the free energy perturbation (FEP) method that is based on the combined scheme of quantum mechanics (QM) and molecular mechanics (MM). The fluctuation and diffusion of the solvent molecules were found to have an important influence on Norrish type reactions of valerophenone. The α C−C bond cleavages were predicted to be not in competition with the 1,5-H shift, which is consistent with the experimental findings that Norrish type II quantum yield is close to unity. The triplet lifetime of aqueous valerophenone was experimentally inferred to be 52 ns, which is nearly reproduced by the QM/MM-FEP calculated rate constant of 2.33×10^7 s^{-1}. The calculated results show that branch ratios of the subsequent reactions from the triplet 1,4-biradical are mainly controlled by the equilibrium populations of its stable conformations. The ratio of cleavage to cyclization measured experimentally is well reproduced by the present QM/MM-FEP calculations. However, the absolute quantum yields of cleavage and cyclization reactions are underestimated theoretically and the reason for this is discussed.

Introduction

The photochemistry of carbonyl compounds has been extensively studied over the past several decades[1−23] and recent studies[17−23] demonstrated that carbonyl compounds continue to play an important role in the development of our understanding of the photochemistry and photophysics of polyatomic molecules. Photoexcitation of a ketone from the ground state to the excited singlet state may lead to breakage of a bond α to the carbonyl group,[1−5] which is known as a Norrish type I reaction.[24] The 1,5-H shift (Norrish type II

(1) Wagner, P. J. *Acc. Chem. Res.* **1971**, *4*, 168–177.
(2) Scaiano, J. C. *Acc. Chem. Res.* **1982**, *15*, 252–258.
(3) Warren, J. A.; Bernstein, E. R. *J. Chem. Phys.* **1986**, *85*, 2365–2367.
(4) Doubleday, C., Jr.; Turro, N. J.; Wang, J. F. *Acc. Chem. Res.* **1989**, *22*, 199–205.
(5) Wagner, P. J. *Acc. Chem. Res.* **1989**, *22*, 83–91.
(6) Zhao, H.-Q.; Cheung, Y.-S.; Liao, C.-L.; Liao, C.-X.; Ng, C. Y.; Li, W.-K. *J. Chem. Phys.* **1997**, *107*, 7230–7241.
(7) Srivastava, S.; Yourd, E.; Toscano, J. P. *J. Am. Chem. Soc.* **1998**, *120*, 6173–6174.
(8) Zepp, R. G.; Gumz, M. M.; Miller, W. L.; Gao, H. *J. Phys. Chem. A* **1998**, *102*, 5716–5723.
(9) Klan, P.; Janosek, J.; Kirz, Z. *J. Photochem. Photobiol., A* **2000**, *134*, 37–44.
(10) Griesbeck, A. G.; Heckroth, H. *J. Am. Chem. Soc.* **2002**, *124*, 396–403.
(11) Fang, W.-H.; Phillips, D. L. *ChemPhysChem* **2002**, *3*, 889–892.
(12) Fang, W.-H.; Phillips, D. L. *J. Theor. Comput. Chem.* **2003**, *2*, 23–31.
(13) Litersk, J.; Klan, P.; Heger, D.; Loupy, A. *J. Photochem. Photobiol., A* **2003**, *154*, 155–159.
(14) He, H.-Y.; Fang, W.-H.; Phillips, D. L. *J. Phys. Chem. A* **2004**, *108*, 5386–5392.
(15) Muller, P.; Loupy, A.; Klan, P. *J. Photochem. Photobiol., A* **2005**, *172*, 146–150.
(16) Ding, L.-N.; Shen, L.; Chen, X.-B.; Fang, W.-H. *J. Org. Chem.* **2009**, *74*, 8956–8962.
(17) Townsend, D.; Lahankar, S. A.; Lee, S. K.; Chambreau, S. D.; Suits, A. G.; Zhang, X.; Rheinecker, J.; Harding, L. B.; Bowman, J. M. *Science* **2004**, *306*, 1158–1161.
(18) Yin, H. M.; Kable, S. H.; Zhang, X.; Bowman, J. M. *Science* **2006**, *311*, 1443–1446.
(19) Houston, P. L.; Kable, S. H. *Proc. Natl. Acad. Sci. U.S.A.* **2006**, *103*, 16079–16082.
(20) Suits, A. G. *Acc. Chem. Res.* **2008**, *41*, 873–881.
(21) Srinivasan, R.; Feenstra, J. S.; Park, S. T.; Xu, S.; Zewail, A. H. *Science* **2005**, *307*, 558–563.
(22) Park, S. T.; Feenstra, J. S.; Zewail, A. H. *J. Chem. Phys.* **2006**, *124*, 174707.
(23) Fang, W.-H. *Acc. Chem. Res.* **2008**, *41*, 452–457.
(24) Norrish, R. G. W.; Appleyard, M. E. S. *J. Chem. Soc.* **1934**, 874–878.

DOI: 10.1021/jo101785z Published on Web 01/11/2011

SCHEME 1. Norrish Type I and II Reactions

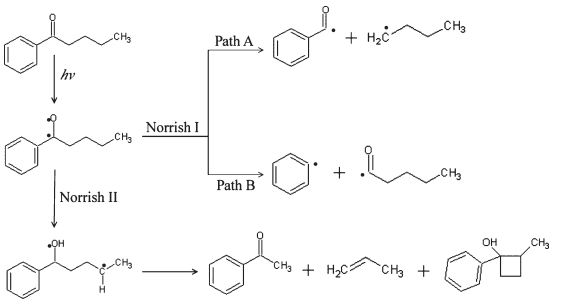

reaction)[24,25] was found to be one of the fundamental photoreactions for ketones that contain a hydrogen atom at the γ-position. It has been well established that Norrish type I and II reactions (Scheme 1) occur from the lowest triplet state for most of the aromatic ketones or aldehydes. The Norrish type II reaction proceeds via a six-member cyclic transition state, leading to formation of a triplet 1,4-biradical as an intermediate. There are three competing pathways for the triplet 1,4-biradical deactivation: the cyclization of the 1,4-biradical to give the cyclobutanol product (Norrish−Yang cyclization), the cleavage of the C−C single bond to produce an enol and the related alkene as products (Norrish II cleavage), and the hydrogen back-transfer to reconstitute the starting material in the ground state.

The structure−reactivity relationship of the 1,4-biradical has been the subject of numerous experimental studies.[26−32] Scheffer and co-workers have investigated effects of geometry and orbital-overlap on the behavior of the 1,4-biradical produced by photolysis of ketones in the crystalline state.[26−28] The 1,5-H shift in the crystalline state occurs with little motion of the associated heavy atoms and the 1,4-biradical structure is determinable by X-ray crystallography of the parent ketones. Conformational effects on the ratio of cyclization to cleavage were explained by overlap between the singly occupied p orbital and the C−C σ^* orbital. Cleavage was found to be favored when the conformation of the 1,4-biradical allows an efficient p−σ^* overlap. The cleavage-to-cyclization ratio has its maximum value at $\beta = 0°$ (β is defined as the angle between the p orbital and the C−C bond).[28] Transient absorption spectroscopy was used to study the lifetime of triplet 1,4-biradicals produced by laser flash photolysis of ketones in different solvents.[2,4,8,29−31] It has been observed that the triplet 1,4-biradical has its lifetimes on the order of tens of nanoseconds for most aromatic alkyl ketones investigated[8,31] and is sufficiently long-lived for equilibrium to be established between the various conformations. In this case, the quantum yields of products are determined to a certain extent by populations of the various conformations of the triplet 1,4-biradical at equilibrium. There exist two subtly different schools of thought concerning the ISC process and the partitioning between cyclization and cleavage.[2,5,10,27,31,33,34] Although the more widely accepted view is that the reactivity of the triplet 1,4-biradical is controlled by intersystem crossing,[2,10,27,31] the spin−orbit coupling (SOC) calculation proved that the SOC matrix elements between the lowest triplet and singlet states are similar for different isomers of the 1,4-biradical.[14,33]

Experimental investigations[1−5,8,26−32] of photoreactions of aromatic alkyl ketones over the past many decades have provided a wealth of information concerning effects of conformational factor and solvent on the 1,4-biradical reactivity. However, there is no clear-cut understanding of how the concerted effect of solvent and conformation on partition of the 1,4-biradical between cyclization and cleavage and the behavior of the 1,4-biradical is still an enigma in general. Attempts to understand the factors that influence the reactivity of triplet 1,4-biradicals continue to be of contemporary interest in view of the importance of the Norrish type reactions in many applications.[10,27,35−37] In the present work, Norrish type reactions of the aqueous valerophenone (VP) have been studied from the viewpoint of theory and more attention was paid to the solvent effect on the conformation of the 1,4-biradical.

Zepp and co-workers have studied kinetics and products of the photoreaction of valerophenone in aqueous solution.[8] The quantum yield of Norrish type II reaction was found to be close to unity in the wavelength region of 290−330 nm and the ratio of cyclization to cleavage was inferred to be about 1:2. On the basis of quenching studies with steady-state irradiations, the triplet lifetime of valerophenone was estimated to be 52 ns. To our knowledge, there is only one report on theoretical investigation of Norrish type II reaction and subsequent processes for valerophenone in water.[16] The electrostatic interactions between the solvent and solute molecules were calculated by a combination of ab initio method (QM) with molecular mechanical force field (MM) and solvent effect on the relative energies was explored by the combined QM/MM calculation.[16] However, the fluctuation and diffusion of solvent molecules leading to different relaxation and barrier-crossing dynamics, which should be described by the free energy calculation, has not been considered in the previous study. The QM/MM-based free energy perturbation method (QM/MM-FEP),[38,39] which has been confirmed to be an accurate and effective method for describing the fluctuation and diffusion effects of solvent molecules for a chemical reaction in solution, is used in the present work for calculating active free energies of Norrish

(25) Yang, N. C.; Yang, D.-D. H. *J. Am. Chem. Soc.* **1958**, *80*, 2913–2914.
(26) Leibovitch, M.; Olovsson, G.; Scheffer, J. R.; Trotter, J. *J. Am. Chem. Soc.* **1998**, *120*, 12755–12769.
(27) Braga, D.; Chen, S.; Filson, H.; Maini, L.; Netherton, M. R.; Patrick, B. O.; Scheffer, J. R.; Scott, C.; Xia, W. *J. Am. Chem. Soc.* **2004**, *126*, 3511–3520.
(28) Yang, C.; Xia, W.; Scheffer, J. R.; Botoshansky, M.; Kaftory, M. *Angew. Chem., Int. Ed.* **2005**, *44*, 5087–5089.
(29) Cai, X.; Cygon, P.; Goldfuss, B.; Griesbeck, A. G.; Heckroth, H.; Fujitsuka, M.; Majima, T. *Chem.—Eur. J.* **2006**, *12*, 4662–4667.
(30) Singhal, N.; Koner, A. L.; Mal, P.; Venugopalan, P.; Nau, W. M.; Moorthy, J. N. *J. Am. Chem. Soc.* **2005**, *127*, 14375–14382.
(31) Moorthy, J. N.; Samanta, S.; Koner, A. L.; Saha, S.; Nau, W. M. *J. Am. Chem. Soc.* **2008**, *130*, 13608–13617.
(32) Ayitou, A. J.-L.; Jesuraj, J. L.; Barooah, N.; Ugrinov, A.; Sivaguru, J. *J. Am. Chem. Soc.* **2009**, *131*, 11314–11315.
(33) Ding, L.-N.; Fang, W.-H. *J. Org. Chem.* **2010**, *75*, 1630–1636.
(34) Wagner, P. J.; Meador, M. A.; Zhou, B.; Park, B. S. *J. Am. Chem. Soc.* **1991**, *113*, 9630–9639.
(35) Natarajan, A.; Mague, J. T.; Ramamurthy, V. *J. Am. Chem. Soc.* **2005**, *127*, 3568–3576.
(36) Roscini, C.; Davies, D. M. E.; Berry, M.; Orr-Ewing, A. J.; Booker-Milburn, K. I. *Angew. Chem., Int. Ed.* **2008**, *47*, 2283–2286.
(37) Herrmann, A. *Angew. Chem., Int. Ed.* **2007**, *46*, 5836–5863.
(38) Hu, H.; Lu, Z.; Yang, W. *J. Chem. Theory Comput.* **2007**, *3*, 390–406. Hu, H.; Yang, W. *Annu. Rev. Phys. Chem.* **2008**, *59*, 573–601.
(39) Zhang, Y.; Liu, H.; Yang, W. *J. Chem. Phys.* **2000**, *112*, 3483–3492.

type reactions of aqueous valerophenone and for simulating isomerization processes of the triplet 1,4-biradical.

Computational Methods

A combined scheme of quantum mechanics (QM) and molecular mechanics (MM) was used in the present work for structural optimizations and subsequent free energy calculations. The total energy of the QM/MM system can be written as follows

$$E = E_{QM} + E_{MM} + E_{QM/MM} \quad (1)$$

where E_{QM} is the quantum mechanical energy of the QM subsystem, and E_{MM} is the standard molecular mechanical interactions involving exclusively atoms in the MM subsystem. Since no covalent interaction exists between the QM and MM subsystems for our aqueous system, the QM/MM interaction can be simplified as

$$E_{QM/MM} = E_{electrostatic} + E_{vdW} \quad (2)$$

In comparison with the electrostatic interaction, E_{vdW} is negligibly small. The sum of E_{QM} and $E_{electrostatic}$ can be obtained with ab initio methods as the eigenenergy of an effective Hamiltonian

$$E_{QM} + E_{electrostatic} = \left\langle \Psi \left| H_{QM} + \sum_{\alpha \in QM} \sum_{\beta \in MM} \frac{Z_\alpha q_\beta}{r_{\alpha\beta}} - \sum_{i}^{N} \sum_{\beta \in MM} \frac{q_\beta}{r_{\beta i}} \right| \Psi \right\rangle \quad (3)$$

where N is the total number of electrons of each QM atom, Z_α is the charge of the nuclei of QM atoms, and q_β is the point charge of MM atoms from the molecular mechanical force field. To save the computational cost, the approximation is introduced during MD simulations that the QM/MM electrostatic interaction can be expressed as

$$E_{electrostatic} = \sum_{\alpha \in QM} \sum_{\beta \in MM} \frac{Q_\alpha q_\beta}{r_{\alpha\beta}} \quad (4)$$

where Q_α is the point charge of QM atoms obtained by fitting the electrostatic potential from the QM calculation. It should be pointed out that Q_α is generated in the mean field of the electrostatic potential from the MM subsystem rather than a particular conformation on account of the fluctuation of MM conformations.[38,39]

An iterative QM and MM optimization procedure[38,39] was used to determine stationary structures of the total system. The structure of the QM subsystem was first optimized at the ab initio level with the fixed structure for the MM subsystem. Once convergence is reached, the electrostatic potential is fitted to obtain the effective charge on each QM atom. Then, the geometric structure of MM subsystem was optimized at the MM level with the QM subsystem fixed at the QM optimized bond parameters. The previous steps are repeated until both meet convergence criteria at the same geometry.

Some advanced approaches such as replica exchange[40,41] and weighted histogram analysis method[41−44] have been developed for the QM/MM free energy calculation, but most of them need to sample different QM conformations on the QM/MM potential energy surface, which requires the enormous computational cost. In comparison, the FEP method is more suitable for computing free energy of photochemical systems in solution, which has been discussed in previous studies.[35,36] For a QM/MM system, the partition function can be represented as

$$Z_0(r_{QM}, r_{MM}) = \int e^{-\beta E(r_{QM}, r_{MM})}\, dr_{QM}\, dr_{MM} \quad (5)$$

where E is the total energy, and r_{QM} and r_{MM} represent coordinates of the QM and MM atoms, respectively. The Helmholtz free energy is related to partition function for an (N, V, T) ensemble as

$$F_0(r_{QM}, r_{MM}) = -\beta^{-1} \ln Z_0(r_{QM}, r_{MM}) \quad (6)$$

Let us consider the free energy as the potential of mean force (PMF) of r_{QM}. The partition function and the Helmholtz free energy can be written as

$$Z(r_{QM}) = \int e^{-\beta E(r_{QM}, r_{MM})}\, dr_{MM} \quad (7)$$

and

$$F(r_{QM}) = -\beta^{-1} \ln Z(r_{QM}) = -\beta^{-1} \ln \int e^{-\beta E(r_{QM}, r_{MM})}\, dr_{MM} \quad (8)$$

The FEP method is commonly used to calculate the difference in free energy between two adjacent conformations (A and B) on the free energy surface[45−47]

$$F_B - F_A = -\beta^{-1} \ln \frac{Z_B}{Z_A} \quad (9)$$

Applying eq 7 into eq 9 it is evaluated as an ensemble average of conformation A or B

$$F_B - F_A = -\beta^{-1} \ln\langle e^{-\beta(E_B - E_A)}\rangle_A = \beta^{-1} \ln\langle e^{\beta(E_B - E_A)}\rangle_B \quad (10)$$

where the broken bracket refers to ensemble averaging. As the second-order approximation to Taylor expansion of eq 10 (also called linear response),[48] the free energy difference can be approximately represented as

$$\Delta F_{AB} = \frac{1}{2}(\langle \Delta E_{AB}\rangle_A + \langle \Delta E_{AB}\rangle_B) - \frac{\beta}{4}[\langle(\Delta E_{AB} - \langle \Delta E_{AB}\rangle_A)^2\rangle_A - \langle(\Delta E_{AB} - \langle \Delta E_{AB}\rangle_B)^2\rangle_B] \quad (11)$$

which is used in our present work. The perturbation is run in both directions, i.e., A → B and B → A, and the difference is a measure of how well ΔF_{AB} is statistically converged. The free energy surface of the triplet 1,4-biradical is calculated as a function of the dihedral angles with a step size of 30° and the free energy difference between two adjacent conformations is comparable to $k_B T$. However, the free energy difference between reactant and transition state for the Norrish type reaction is very large. Several conformations on the pathway from reactant to

(40) Sugita, Y.; Kitao, A.; Okamoto, Y. *J. Chem. Phys.* **2000**, *113*, 6042–6051.
(41) Babin, V.; Sagui, C. *J. Chem. Phys.* **2010**, *132*, 104108.
(42) Ferrenberg, A. M.; Swendsen, R. H. *Phys. Rev. Lett.* **1989**, *63*, 1195–1198.
(43) Kumar, S.; Bouzida, D.; Swendsen, R. H.; Kollman, P. A.; Rosenberg, J. M. *J. Comput. Chem.* **1992**, *13*, 1011–1021.
(44) Roux, B. *Comput. Phys. Commun.* **1995**, *91*, 275–282.
(45) Straatsma, T. P.; Berendsen, H. J. C.; Postma, J. P. M. *J. Chem. Phys.* **1986**, *85*, 6720–6727.
(46) Mezei, M. *J. Chem. Phys.* **1987**, *86*, 7084–7088.
(47) Straatsma, T. P.; McCammon, J. A. *J. Chem. Phys.* **1991**, *95*, 1175–1188.
(48) Levy, R. M.; Belhadi, M.; Kitchen, D. B. *J. Chem. Phys.* **1991**, *95*, 3627–3633.

transition state are selected as intermediate states and the final barrier is the sum over free energy differences between two neighboring states. Once the activation free energy is calculated by the FEP method, the rate constant is easily estimated from transition state theory (TST),[49−51]

$$k_{TST} = \frac{k_B T}{h} e^{-\Delta G/RT} \quad (12)$$

To mimic the nature of valerophenone in the water environment, we built a water box of 40 × 40 × 40 Å^3 including 2219 water molecules with the VP enclosed. Then the VP molecule is treated as the QM subsystem, while the remaining atoms are calculated at the molecular mechanical level utilizing the OPLS-AA/L all-atom force field.[52−58] For the explicit solvent simulations the TIP3P water[59] model is used. The ESP charges of QM atoms are computed with a QM/MM simulation of 300 ps, which consists of 100 ps of equilibration and 200 ps of sampling.[38,39,60,61] The free energy differences are calculated by the FEP method from an MD sampling of 1000 ps with the QM geometry and ESP charges frozen. Many independent MD simulations have been performed with different initial settings to determine relative free energies of stationary structures on the pathways of Norrish type reactions and 1,4-biradical isomerization. Each MD simulation is carried out with a time step of 1.0 fs. Periodic boundary conditions are used for the MD simulation. The temperature of the whole system is kept at 300 K by a Berendsen thermostat.[62] The cutoff of 10 Å is set to treat the nonbonded interactions. The B3LYP method is chosen for the present QM calculation because it has proved to be computationally efficient in the treatment of rather large systems in the ground and lowest triplet states and can provide a satisfactory reproduction of the observed stable structures and their relative energies.[14,16,63−66] The nature of all stationary points reported here is confirmed by an analytical frequency computation at the B3LYP/6-311G** level. All calculations are implemented by the Gaussian 03 package[67] that linked to the Gromacs-3.3 package.[68]

Results and Discussion

Norrish Type I and II Reactions. The $S_1(^1n\pi^*) \rightarrow T_1(^3n\pi^*)$ intersystem crossing was confirmed to occur very efficiently due to the existence of the $S_1(^1n\pi^*)/T_1(^3n\pi^*)/T_2(^3\pi\pi^*)$ intersection for valerophenone.[16] Both Norrish type I and II reactions proceed along the lowest triplet state pathways, which have been observed for most aromatic ketones.[1−5,14,16,23,33] In the previous study,[16] the structures and relative energies of the ground state (S_0) and the lowest triplet state (T_1) of valerophenone in water have been calculated by the iterative QM/MM optimization, which mainly includes the Coulomb interactions between the solvent and solute molecules. Here we compute the relative free energy based on the QM/MM optimized S_0 and T_1 equilibrium structures and explore the influence of fluctuation and diffusion of the solvent molecules. The relative energy of the T_1 state was predicted to be 69.5 kcal·mol^{-1} for the VP molecule in the gas phase and increased to 72.5 kcal·mol^{-1} for the molecule in water solution. The present QM/MM-FEP calculations predict that the T_1 structure has its relative free energy of 67.1 kcal·mol^{-1}, which is lower than its relative energy.

The VP−H_2O complex was treated as the QM subsystem in the previous QM/MM calculations[16] and the B3LYP/6-311G** calculation for the QM subsystem provides the information on the H-bond character between VP and H_2O. It was found that the H-bond interaction between VP and H_2O originates mainly from a donation of the lone-pair electrons of the carbonyl O atom of VP to the H−O σ^* orbital of H_2O from the viewpoint of valence-bond theory. One of the lone-pair electrons is excited to the C=O π^* orbital in the $T_1(^3n\pi^*)$ state, which leads to a decrease of the electron density on the carbonyl O atom. As a result, the intermolecular H-bond is significantly weakened in the $T_1(^3n\pi^*)$ state, as compared with that in the S_0 state. On the one hand, the S_0 state is stabilized more than the T_1 state by the H-bonding interaction between VP and H_2O, which is mainly responsible for an increase of the T_1 relative energy from the gas phase to aqueous solution. On the other hand, the system becomes more flexible in the T_1 state due to weaker H-bonding interaction between VP and H_2O, which is the main reason why the relative free energy is decreased for the system in the T_1 state. The evidence for this comes from the QM/MM-FEP calculated entropy increase of 0.018 kcal·mol^{-1}·K^{-1} in the $S_0 \rightarrow T_1$ process.

The activation free energies on the T_1 state were calculated with the QM/MM-FEP method for Norrish type I and II reactions by using the QM/MM optimized stationary structures on the T_1 state. The obtained results are summarized in Table 1 and Figure 1. There are two C−C bonds α to the carbonyl group for valerophenone. The α C−C bond cleavage along the T_1 pathway can lead to fragments of PhCO + $CH_2CH_2CH_2CH_3$ (path A) or Ph + $COCH_2CH_2CH_2CH_3$ (path B) via the transition state of TS1A or TS1B. The active free energy was predicted to be 15.3 and 28.9 kcal·mol^{-1} for path A and path B, respectively. It can be expected that the α C−C bond cleavage along path B takes place more difficultly than the cleavage along path A, due to the conjugated interaction between the carbonyl group and phenyl ring.

(49) Eyring, H. *J. Chem. Phys.* **1934**, *3*, 107–115.
(50) Wigner, E. *Trans. Faraday Soc.* **1938**, *34*, 29–41.
(51) Hänggi, P.; Talkner, P.; Borkovec, M. *Rev. Mod. Phys.* **1990**, *62*, 251–341.
(52) Jorgensen, W. L.; Maxwell, D. S.; Tirado-Rives, J. *J. Am. Chem. Soc.* **1996**, *118*, 11225–11236.
(53) McDonald, N. A.; Jorgensen, W. L. *J. Phys. Chem. B* **1998**, *102*, 8049–8059.
(54) Jorgensen, W. L.; McDonald, N. A. *J. Mol. Struct.* (*THEOCHEM*) **1998**, *424*, 145–155.
(55) Rizzo, R. C.; Jorgensen, W. L. *J. Am. Chem. Soc.* **1999**, *121*, 4827–4836.
(56) Price, M. L. P.; Ostrovsky, D.; Jorgensen, W. L. *J. Comput. Chem.* **2001**, *22*, 1340–1352.
(57) Watkins, E. K; Jorgensen, W. L. *J. Phys. Chem. A* **2001**, *105*, 4118–4125.
(58) Kaminski, G. A.; Friesner, R. A.; Tirado-Rives, J.; Jorgensen, W. L. *J. Phys. Chem. B* **2001**, *105*, 6474–6487.
(59) Jorgensen, W. L.; Chandrasekhar, J.; Madura, J. D.; Impey, R. W.; Klein, M. L. *J. Chem. Phys.* **1983**, *79*, 926–935.
(60) Besler, B. H.; Merz, K. M., Jr.; Kollman, P. A. *J. Comput. Chem.* **1990**, *11*, 431–439.
(61) Lu, Z.; Yang, W. *J. Chem. Phys.* **2004**, *121*, 89–100.
(62) Berendsen, H. J. C.; Postma, J. P. M.; van Gunsteren, W. F.; DiNola, A.; Haak, J. R. *J. Chem. Phys.* **1984**, *81*, 3684–3690.
(63) Lee, C.; Yang, W.; Parr, R. G. *Phys. Rev. B* **1988**, *37*, 785–789.
(64) Becke, A. D. *J. Chem. Phys.* **1993**, *98*, 5648–5652.
(65) Pople, J. A.; Gill, P. M. W.; Handy, N. C. *Int. J. Quantum Chem.* **1995**, *56*, 303–305.
(66) Curtiss, L. A.; Raghavachari, K.; Redfern, P. C.; Pople, J. A. *J. Chem. Phys.* **1997**, *106*, 1063–1079.
(67) Frisch, M. J. et al. *Gaussian 03*, Revision C.02; Gaussian, Inc.: Pittsburgh, PA, 2003.
(68) GROMACS is free software for molecular simulation and trajectory analysis, which is written by van der Spoel, D. and co-workers in the GROMACS development team in Netherlands. Gromacs Version 3.3 is used in this study.

TABLE 1. Relative Energies and Free Energies (kcal·mol^{-1}) for Stationary Structures in the T_1 State, along with Rate Constants (s^{-1}) of Norrish Type I and II Reactions

	energy			
	in vacuum	in aqueous	free energy in aqueous	rate constant in aqueous
VP-T_1	0.0	0.0	0.0	
TS1A	16.6	14.5	15.3	5.27×10^{1}
TS1B	28.7	20.4	28.9	7.54×10^{-9}
TS2	3.8	0.6	7.5	2.33×10^{7}

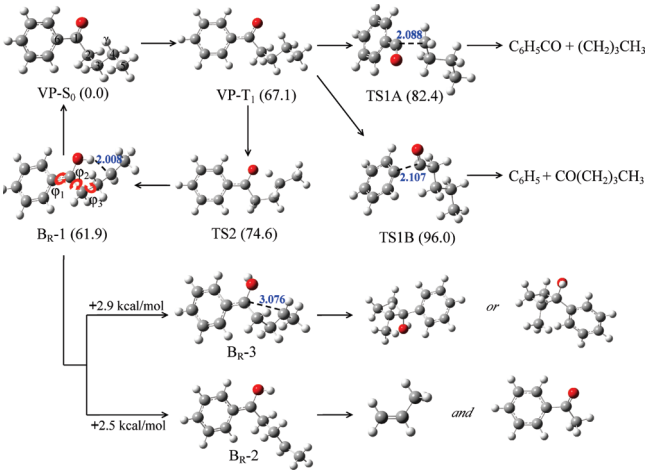

FIGURE 1. Stationary structures and their relative free energies (kcal·mol^{-1} in parentheses) on pathways of Norrish type reactions and the subsequent processes from the triplet 1,4-biradical, along with the selected bond distances (Å) and the atom-labeling scheme illustrated in the VP-S_0 structure.

This is in good agreement with the calculated active free energies. Applying the calculated active free energies into eq 12, the two α C−C bond cleavages were calculated to have rate constants of 7.54×10^{-9} and 5.27×10^{1} s^{-1}, respectively.

The 1,5-H shift (Norrish type II reaction) along the T_1 pathway gives rise to a 1,4-biradical as an intermediate through a six-membered ring transition state (TS2). The active free energy was predicted to be 7.5 kcal·mol^{-1} by the QM/MM-FEP calculations, which is much lower than the active free energies of 15.3 and 28.9 kcal·mol^{-1} on the pathways of the α C−C bond cleavages. The rate constant of the 1,5-H shift reaction was calculated to be 2.33×10^{7} s^{-1} by using eq 12. It should be pointed out that the calculated active free energies of 7.5 kcal·mol^{-1} for the 1,5-H shift is higher than the energy barrier of 0.6 kcal·mol^{-1} reported in the previous study.[16] This should be attributed to entropy decrease in the process from the T_1 equilibrium structure (VP-T_1) to the transition state (TS2) for the 1,5-H shift reaction. The conformational change from VP-T_1 to TS2 for the QM subsystem has a considerable contribution to entropy decrease, which was estimated by normal vibrational analyses for the isolated VP-T_1 molecule and TS2 structure. It was found that the entropy is decreased by 0.007 kcal·mol^{-1}·K^{-1}, giving rise to an increase of the active free energy by 2.1 kcal·mol^{-1} at 300 K. The energy barrier of 0.6 kcal·mol^{-1} was calculated by the iterative QM/MM optimization, which is only based on one minimum-energy structure for the MM subsystem and the solvent fluctuation was not considered in the previous study.[16] The contribution of the solvent fluctuation to entropy decrease was calculated by the QM/MM-FEP calculation with the QM subsystem fixed at the QM/MM optimized structure. The entropy was estimated to decrease by 0.015 kcal·mol^{-1}·K^{-1} from VP-T_1 to TS2, due to the solvent fluctuation.

Upon inspection of the calculated rate constants listed in Table 1, it can be seen that the α C−C bond cleavages are not in competition with the 1,5-H shift, which is consistent with the experimental findings that Norrish type II quantum yield is close to unity throughout the 290−330 nm spectral region.[8] In addition, on the basis of quenching studies with steady-state irradiation, the triplet lifetime of aqueous valerophenone at 20 °C was experimentally estimated to be 52 ns. The corresponding rate constant of 1.92×10^{7} s^{-1} (52 ns) is very close to the calculated value of 2.33×10^{7} s^{-1}. It is evident that the triplet lifetime is mainly controlled by the 1,5-H shift reaction for valerophenone in aqueous solution. More importantly, a good agreement between experiment and theory provides the strong evidence that Norrish type II reaction of aqueous valerophenone can be well described by the QM/MM-FEP calculations.

Conformations of 1,4-Biradical and the Subsequent Reactions. Experimentally, it has been observed that the triplet 1,4-biradical is sufficiently long-lived for equilibrium to be established between the various conformations for most aromatic alkyl ketones investigated.[8,31] Thus, the branch ratios of the subsequent reactions are determined to a large extent by the equilibrium populations of the triplet conformations. Twelve structures for the 1,4-biradical in aqueous solution were characterized by the iterative QM/MM optimization and were confirmed to be minima on the triplet potential energy surface by the frequency calculations. Isomerization processes among the twelve isomers involve mainly the rotations around the C−C single bonds, which can be described by a change in the C6−C1−C2−C3 (φ_1), C1−C2−C3−C4 (φ_2), and C2−C3−C4−C5 (φ_3) dihedral angles. The optimized bond parameters for these isomers and their relative energies are listed in Table 2. As can be seen from the optimized structures in Figure 1, B_R-1 has a favorable conformation for the hydrogen back-transfer to reconstitute the parent ketone after ISC to the lowest singlet state, referred to as type-1 in Table 2. Because of an efficient overlap between the singly occupied p orbital at the C1 atom and the C2−C3 σ^* orbital, B_R-2 is well aligned for Norrish II cleavage, referred to as type-2. The B_R-3 isomer exhibits a tendency to undergo the Norrish−Yang cyclization, due to a short C1−C4 distance, and is referred to as type-3.

The C1−C4 distance in B_R-4 (3.144 Å) is a little longer than that (3.067 Å) in B_R-3 and the difference in the C6−C1−C2−C3 angle between B_R-3 and B_R-4 is close to 180°. Like B_R-3, B_R-4 has a favorable conformation for the Norrish−Yang cyclization. The C4−Hγ distance in B_R-5 is very short (2.833 Å) and can be referred to as type-1, although the C6−C1−C2−C3 and C2−C3−C4−C5 angles are quite different in B_R-5 and B_R-1. Isomers from B_R-6 to B_R-12 mainly originate from the terminal CH_3 rotation (φ_3) of B_R-1, B_R-2, and B_R-3, which are labeled as type-1, type-2, and type-3 in Table 2 in line with the related reactions. It can be expected that the terminal CH_3 rotation has little influence on the branch ratio of the subsequent reactions of the 1,4-biradical. In addition, these isomers have relatively high

TABLE 2. Dihedral Angles (deg) and Relative Energies (kcal·mol^{-1}) for the Stable Triplet 1,4-Biradical Isomers

	C6−C1−C2−C3	C1−C2−C3−C4	C2−C3−C4−-C5	rel energy
B_R-1 (type-1)	−153.4	−69.7	165.1	0.0
B_R-2 (type-2)	−81.5	176.4	166.4	0.9
B_R-3 (type-3)	79.9	58.5	−162.6	4.1
B_R-4 (type-3)	−120.6	62.5	−166.4	3.8
B_R-5 (type-1)	−103.1	−67.6	−151.3	1.9
B_R-6 (type-1)	−142.2	−66.1	−69.0	5.8
B_R-7 (type-2)	−60.2	175.2	−81.3	6.9
B_R-8 (type-2)	67.7	−170.6	157.6	7.3
B_R-9 (type-3)	−116.3	61.7	77.1	6.4
B_R-10 (type-3)	−126.2	59.1	85.1	6.4
B_R-11 (type-3)	−107.5	53.9	−89.1	6.6
B_R-12 (type-3)	−121.3	69.2	−160.5	11.0

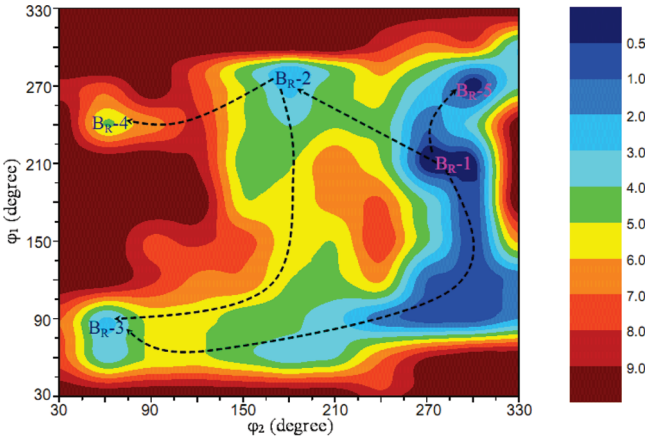

FIGURE 2. The relative free energies (kcal·mol^{-1}) are plotted as a function of the C6−C1−C2−C3 (φ_1) and C1−C2−C3−C4 (φ_2) dihedral angles for the triplet 1,4-biradical in aqueous solution with the isomerization pathways shown by dashed lines.

energies and their populations are very small at thermal equilibrium with respect to B_R-*i* (*i* = 1−5). The B_R-1 conformation is the most stable with the relative energies of 0.9 and 4.1 kcal·mol^{-1} for B_R-2 and B_R-3, respectively.

Here we pay more attention to the stable conformations of the 1,4-biradical in the T_1 free energy surface. As discussed above, the conformational isomerization that controls the ratio of different products is determined by the C6−C1−C2−C3 (φ_1) and C1−C2−C3−C4 (φ_2) dihedral angles. On the basis of the optimized conformations for the triplet 1,4-biradical, the triplet free energy surface was calculated as a function of the φ_1 and φ_2 dihedral angles with the QM/MM-FEP method. The φ_1 and φ_2 angles were changed from 0° to 360° with a step-size of 30°. To obtain the smooth plot for the free energy surface, free energies were calculated for a lot of additional φ_1 and φ_2 values. The two-dimensional contour of the calculated free energy surface is plotted in Figure 2, which reflects the conformational isomerization of the triplet 1,4-biradical in aqueous solution. As shown in Figure 2, five local minima were found on the free energy surface and their structures are very similar to those in the potential energy surface. This gives us a hint that the optimized stationary structures on potential energy surface can be approximately used for free energy calculations. As can be seen from Figure 2, the free energy of the system is nearly unchanged when the φ_1 angle is decreased from 210° to 90° with the φ_2 angle fixed at ∼290°. However, free energy of the system is increased by ∼4.5 kcal/mol when the φ_2 angle varies from 270° to 100° with the φ_1 angle fixed at ∼90°. The φ_2 angle can be considered as the reaction coordinate and its change is tightly related isomerization from B_R-1 to B_R-2 or B_R-3. Thus, a large change of free energy with the φ_2 angle predicts that the hydrophobic interaction between VP and water can have a significant effect on the isomerization processes.

TABLE 3. Free Energy Diffenerces and Barriers (kcal·mol^{-1}) for Isomerization Pathways of the Four Stable Isomers of the Triplet 1,4-Biradical in Aqueous Solution and the Corresponding Rate Constants (s^{-1})

reactant	product	free energy difference	free energy barrier	rate constant
B_R-1	B_R-2	2.5	4.9	1.8×10^9
B_R-1	B_R-3	2.9	5.3	9.1×10^8
B_R-2	B_R-3	0.4	3.0	4.2×10^{10}
B_R-2	B_R-4	2.4	5.8	4.0×10^8

The B_R-1 conformation is the most stable structure on the triplet free energy surface, which is similar to that on the triplet potential energy surface. The relative free energies of B_R-2, B_R-3, B_R-4, and B_R-5 are respectively 2.5, 2.9, 4.9, and 0.1 kcal·mol^{-1} with respect to the B_R-1 minimum. Isomerization pathways of five different conformations are shown with dashed lines in Figure 2. As listed in Table 3, the free energy barriers from B_R-1 to B_R-2 and B_R-3 were calculated to be 4.9 and 5.3 kcal·mol^{-1}, respectively, while the isomerizations from B_R-2 to B_R-3 and B_R-4 have the free energy barriers of 3.0 and 5.8 kcal·mol^{-1}, respectively. Applying these free energy barriers into eq 12, isomerization processes from B_R-1 to B_R-2 and B_R-3, and from B_R-2 to B_R-3 and B_R-4 have rate constants of 1.8×10^9, 9.1×10^8, 4.2×10^{10}, and 4.0×10^8 s^{-1}, respectively.

The spin-conservation reactions from the triplet 1,4-biradical were confirmed to take place with little probability, due to relatively high barriers or high endothermicity.[14,16,33] Thus, intersystem crossing (ISC) from the triplet 1,4-biradical to the singlet state might play an important role in the subsequent reactions. The ISC rate constant was predicted to be ∼10^7 s^{-1} from the triplet 1,4-biradical to its singlet state for butyrophenone and acetylphenylacetic acid by nonadiabatic RRKM rate calculations,[14,33] which is consistent with the lifetime of about 10^{-7} s measured for the several triplet 1,4-biradicals in the solution phase.[69] Since the triplet−singlet ISC rate constant (∼10^7 s^{-1}) is much smaller than those (∼10^9) for the isomerization processes among different conformations of the triplet 1,4-biradical, thermal equilibrium can be established among the five stable conformations of the triplet 1,4-biradical, which is in a good agreement with the experimental findings.[8,31] The singlet 1,4-biradical is very reactive, thus the subsequent cleavage, cyclization, and hydrogen back-transfer proceed very easily once the singlet 1,4-biradical is formed by intersystem crossing from the triplet 1,4-biradical. Therefore, branch ratios of the subsequent reactions are determined to large extent by the equilibrium populations of the triplet conformations.

The B_R-4 conformation has its relative free energy of 4.9 kcal·mol^{-1} with respect to the B_R-1 minimum and the B_R-4 equilibrium population is less than 0.1% of that for the B_R-1 conformation. Therefore, the B_R-4 conformation has a

(69) Das, P. K.; Encinas, M. V.; Small, R. D., Jr.; Scaiano, J. C. *J. Am. Chem. Soc.* **1979**, *101*, 6965–6970.

negligible contribution to the subsequent reactions. The relative free energy of B_R-3 is 0.4 kcal·mol^{-1} higher than that for B_R-2, and the B_R-2:B_R-3_1 population ratio is close to 2:1 at thermal equilibrium. As pointed out before, B_R-2 is well aligned for the Norrish II cleavage, due to an efficient p−σ* overlap, and B_R-3 has an optimal geometry for the Norrish−Yang cyclization. Thus, the B_R-2:B_R-3 population ratio at thermal equilibrium is approximately equal to the cleavage:cyclization branch ratio. The quantum yields were inferred to be 0.65 for the cleavage and 0.32 for the cyclization upon photoexcitation of aqueous valerophenone.[8]

As can be seen from Figure 1, B_R-1 is well set up for the hydrogen back-transfer, which reveals that the disproportionation back to the starting ketone is a dominant pathway after formation of the 1,4-biradical. However, the sum of cyclization and cleavage quantum yields was calculated to be close to unity by using the estimated first-order rate constant and the molar absorptivity integrated over all the effective wavelengths of the light source.[8] Since an aqueous solution of valerophenone was irradiated for a long time in the kinetics study, the parent ketone, which is formed by the disproportionation of the 1,4-biradical, can be re-excited and followed by the Norrish type II reaction. This might be one of the reasons that quantum yields of cyclization and cleavage reactions were overestimated experimentally. The relative free energies of B_R-2 and B_R-3 may be overestimated by ∼2.0 kcal·mol^{-1} with the QM/MM-FEP calculation, which is the reason that the absolute quantum yields of the cyclization and cleavage are underestimated theoretically. More accurate calculation of the relative free energies is still a challenging task for the current quantum chemical methods.

Summary

In the present work, the QM/MM-based free energy perturbation (FEP) method has been used to study Norrish type reactions of aqueous valerophenone and the behavior of the triplet 1,4-biradical formed by the Norrish type II reaction. On the basis of the QM/MM-FEP calculated active free energies, the rate constants were estimated with transition state theory. The Coulomb interactions between the solvent and solute molecules and the fluctuation and diffusion of the solvent molecules were found to have an important influence on the α C−C bond cleavage and the 1,5-H shift reactions of valerophenone and the relative stability of different isomers of the triplet 1,4-biradical. The calculated active free energies reveal clearly that the α C−C bond cleavages are not in competition with the 1,5-H shift, which is consistent with the experimental findings that Norrish type II quantum yield is close to unity throughout the 290−330 nm spectral region. In addition, the triplet lifetime of aqueous valerophenone at 20 °C was experimentally estimated to be 52 ns (the corresponding rate constant of 1.92×10^7 s^{-1}), which is comparable with the calculated rate constant of 2.33×10^7 s^{-1} for the Norrish type II reaction. A good agreement between experiment and theory provides the evidence that Norrish type reactions of aqueous valerophenone can be well described by the QM/MM-FEP calculations.

The five most stable conformations for the 1,4-biradical in the triplet free energy surface were determined by the QM/MM-FEP calculations. Rate constants for isomerization processes among the five different conformations were estimated from transition state theory, which are much larger than the ISC rates from the triplet to singlet 1,4-biradical. This shows that the thermal equilibrium can be established among the five stable conformations of the triplet 1,4-biradical. In this case, branch ratios of the subsequent reactions are mainly controlled by the equilibrium populations of the triplet stable conformations. The ratio of cleavage to cyclization was experimentally measured to be about 2:1 upon photoexcitation of aqueous valerophenone at 290−330 nm, which is well reproduced by the present QM/MM-FEP calculations. The disproportionation back to the starting ketone was predicted to be a dominant pathway after formation of the 1,4-biradical. However, the quantum yields were measured to be about 0.65 for the cleavage and 0.32 for the cyclization. The parent ketone formed by the disproportionation of the 1,4-biradical can be re-excited and followed by the Norrish type II reaction, which might be one of the reasons that quantum yields of cyclization and cleavage reactions were overestimated experimentally. The relative free energies of the stable isomers of the triplet 1,4-biradical are a little overestimated by the QM/MM-FEP calculation and this is the reason that the absolute quantum yields of the cyclization and cleavage are underestimated theoretically.

Acknowledgment. This work was supported by grants from the NSFC (Grant No. 20720102038) and from the Major State Basic Research Development Programs (Grant No. 2010CB808503).

Supporting Information Available: Cartesian coordinates and absolute energies of the stationary structures. This material is available free of charge via the Internet at http://pubs.acs.org.